

# Reuse Within a Cell—Interference Rejection or Multiuser Detection?

Claes Tidestav, *Student Member, IEEE*, Mikael Sternad, *Senior Member, IEEE*,  
and Anders Ahlén, *Senior Member, IEEE*

**Abstract**—We investigate the use of an antenna array at the receiver in frequency-division multiple-access/time-division multiple-access systems to let several users share one communication channel within a cell. A decision-feedback equalizer (DFE) which simultaneously detects all incoming signals is compared to a set of DFE's, each detecting one signal and rejecting the remaining as interference. We also introduce the existence of a zero-forcing solution to the equalization problem as an indicator of near-far resistance of different detector structures. Near-far resistance guarantees good performance if the noise level is low.

Simulations show that with an increased number of users in the cell, the incremental performance degradation is small for the multiuser detector. We have also applied the proposed algorithms to experimental measurements from a DCS-1800 antenna array testbed. The results from these experiments confirm that reuse within a cell is indeed possible using either an eight-element array antenna or a two-branch diversity sector antenna. Multiuser detection will, in general, provide better performance than interference rejection, especially when the power levels of the users differ substantially. The difference in performance is of crucial importance when the available training sequences are short.

**Index Terms**—Antenna arrays, decision-feedback equalizers, interference suppression, multiuser channels, multivariable systems.

## I. INTRODUCTION

**I**N A WIRELESS cellular communication system, multi-element antennas, also known as *antenna arrays*, can be used at the receiver to increase the system capacity. Antenna arrays can enhance the desired signal and suppress the interference so that the radio spectrum can be used more frequently across the network, thereby decreasing the so-called *reuse factor*. When all frequencies are utilized in every cell, the system is said to have reuse factor one.

To increase the capacity of a frequency-division multiple-access or time-division multiple-access (TDMA) cellular system which has reuse factor one, several users within a cell would have to share each of the available frequencies and time slots; the system must support *reuse within a cell*.<sup>1</sup>

Paper approved by C.-L. Wang, the Editor for Equalization of the IEEE Communications Society. Manuscript received June 10, 1998; revised November 4, 1998 and March 5, 1999. This paper was presented in part at the 49th IEEE Vehicular Technology Conference, Houston, TX, May 16–20, 1999, and at the Radiovetenskap och Kommunikation 99, Karlskrona, Sweden, June 14–17, 1999.

The authors are with the Signals and Systems Group, Uppsala University, Uppsala SE-751 20, Sweden (e-mail: Claes.Tidestav@signal.uu.se).

Publisher Item Identifier S 0090-6778(99)07795-8.

<sup>1</sup>This concept is also known as spatial-division multiple-access or SDMA.

This will cause severe cochannel interference (CCI) at the receiver. Antenna arrays are then indispensable tools for separating the signals from different users. With an antenna array, beamforming [1] can be used to suppress CCI. However, in situations with frequency selective fading, beamformers that operate only in the spatial domain can suppress only a few interferers. In this paper, we illustrate, compare, and explore two more elaborate ways of using an antenna array at the receiver to accomplish reuse within a cell.

- 1) Detect the signal from one user at a time while treating the other users as interference. In the following, this approach will be denoted *interference rejection* or *interference cancellation*.
- 2) Detect the signals from all users simultaneously, which will be called *multiuser detection*.

Interference rejection using linear receivers is studied in [2], whereas decision-feedback equalizers (DFE's) are used for the same purpose by Monsen in [3] and Balaban and Salz in [4]. DFE's are also the topic of [5], but in an adaptive setting. In [6], Bottomley and Jamal use maximum-likelihood sequence estimation (MLSE) with spatial interference whitening to suppress ISI and CCI. Interference rejection, i.e., taking the covariance matrix of the interference into account, leads to substantial performance improvements in all these papers.

Multiuser detection within a cell using antenna arrays was first suggested by Winters in [7] and [8]. The emphasis of these papers is on frequency *nonselective* channels and linear detectors. In [9], extensions are made to frequency selective channels. Linear and nonlinear multiuser detectors have been extensively investigated for application in code-division multiple-access (CDMA) systems (see, e.g., [10]–[14]).

As will become evident in the following sections, the performance of multiuser detectors is mostly superior to that of interference cancellers. This is due to two reasons.

- 1) Nonlinear multiuser detectors can suppress interference more efficiently than nonlinear interference cancellers. (This is in contrast to mean-square error (MSE) optimal *linear* detectors, such as those used in [8]. A MSE-optimal linear multiuser detector is exactly the same detector as a set of MSE-optimal linear interference cancellers.)
- 2) The channel estimation is improved. When utilizing training sequences from all users instead of treating all except one as noise, the estimates of channel and noise statistics will be based on more data. Therefore, the

model quality is, in general, improved, which leads to more precise tuning of the detector.

In this paper we will use DFE's to illustrate the influence of these two factors. Throughout the paper, we will compare two equalizer structures.

- 1) The DFE presented in [5], which rejects interference.
- 2) The DFE of [15], which detects multiple signals simultaneously.<sup>2</sup>

These algorithms will be compared and studied by analysis in Section III and by extensive simulations in Section IV. In Section V, we apply the algorithms to experimental data collected at an antenna array testbed.

## II. CHANNEL MODELS

We shall now introduce the channel models upon which we base the derivation of the detectors. These baseband models are assumed to be linear and sampled at the symbol rate.<sup>3</sup> They are also assumed to include the effects of pulse shaping and analog modulation. The symbol rate is equal for all users. Finally, we assume the channel models to be *time-invariant* over the duration of a TDMA burst. The motivation for the last assumption is solely for simplicity of presentation.

### A. Multiple-Input Multiple-Output (MIMO) Baseband Channel Model

We consider a case with  $M$  transmitters and  $N$  receiver antennas. In the uplink,<sup>4</sup> the  $M$  transmitters represent  $M$  different mobiles, each being equipped with one antenna. Each mobile transmits a signal to the base station, which uses an  $N$  element antenna array to detect all the signals. For downlink transmission,<sup>5</sup> we assume that the base station is equipped with  $M$  antennas, each of which transmits a separate message. Each mobile has  $N$  receiver antennas, which are used to detect one (or several) of the transmitted signals.

The signal from transmitter  $j$  propagates through the discrete-time baseband channel  $H_{ij}(z^{-1})$  to receiver antenna  $i$ . The channel  $H_{ij}(z^{-1})$  is given by

$$H_{ij}(z^{-1}) = H_{ij}^0 + H_{ij}^1 z^{-1} + \dots + H_{ij}^{L_{ij}} z^{-L_{ij}} \quad (1)$$

where  $H_{ij}^n$  are complex-valued constants and where  $z^{-1}$  represents the unit delay operator.<sup>6</sup>

The digital signal received at antenna  $i$  at the discrete time instant  $k$  is denoted  $x_i(k)$  and can be expressed as

$$x_i(k) = \sum_{n=1}^M H_{in}(z^{-1}) s_n(k) + v_i(k) \quad (2)$$

<sup>2</sup>This minimum-mean square error (MMSE) DFE was first derived in [16] and independently in [17]. It resembles the DFE presented in [18] but is derived under the constraint of *realizability* (finite decision delay and causal filters) and generalized for straightforward application to channels with different number of inputs and outputs.

<sup>3</sup>Since the bandwidth of the signal is at least as large as the reciprocal of the symbol rate, symbol rate sampling actually constitutes *undersampling*.

<sup>4</sup>Transmission from the mobile to the base station, also known as the reverse link.

<sup>5</sup>Transmission from the base station to the mobile, also known as the forward link.

<sup>6</sup>For any signal  $y(k)$ ,  $z^{-1}y(k) = y(k-1)$ .

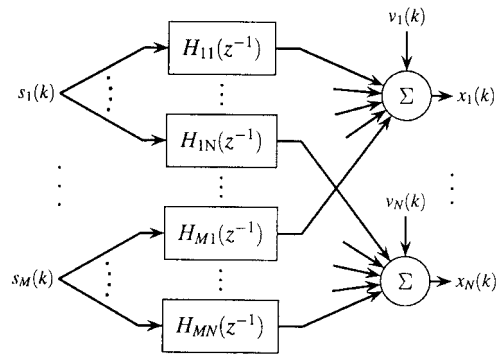


Fig. 1. The MIMO channel model where  $s_j(k)$  is the symbol transmitted at discrete-time instant  $k$  from user number  $j$ , while  $x_i(k)$  is the received sampled baseband signal at antenna  $i$ . The signal  $v_i(k)$  represents additive noise and out-of-cell CCI.

where  $s_j(k)$  is the symbol transmitted from user  $j$  and the term  $v_i(k)$  corresponds to noise and out-of-cell CCI. The signals  $s_j(k)$  and the noises  $v_i(k)$  are assumed to be mutually uncorrelated, zero-mean wide-sense stationary stochastic signals. Furthermore, all signals  $s_j(k)$ ,  $j = 1, \dots, M$ , are assumed to be mutually uncorrelated and white with zero mean. The situation is depicted in Fig. 1.

To obtain a MIMO model, we introduce the signal vectors

$$x(k) = (x_1(k) \ x_2(k) \ \dots \ x_N(k))^T \quad (3a)$$

$$s(k) = (s_1(k) \ s_2(k) \ \dots \ s_M(k))^T \quad (3b)$$

$$v(k) = (v_1(k) \ v_2(k) \ \dots \ v_N(k))^T. \quad (3c)$$

The vector  $v(k)$  of noise samples is characterized by the matrix-valued covariance function

$$\psi_{k-m} \triangleq E[v(k)v^H(m)]. \quad (4)$$

The vector  $x(k)$  of sampled antenna outputs can now be expressed as

$$x(k) = \mathbf{H}(z^{-1})s(k) + v(k) \quad (5)$$

$$= \mathbf{H}_0 s(k) + \dots + \mathbf{H}_L s(k-L) + v(k) \quad (6)$$

where we have introduced the MIMO impulse response

$$\mathbf{H}(z^{-1}) = \begin{pmatrix} H_{11}(z^{-1}) & \dots & H_{1M}(z^{-1}) \\ \vdots & \ddots & \vdots \\ H_{N1}(z^{-1}) & \dots & H_{NM}(z^{-1}) \end{pmatrix} \quad (7)$$

with individual matrix coefficients (taps)  $\mathbf{H}_p$ . In (6),  $L = \max_{i,j} L_{ij}$  represents the maximum order of all scalar channels (1).

*Remark 1:* Although the focus of this paper will be on reuse within a cell, out-of-cell interferers communicating with other base stations could be included among the  $M$  users, which are explicitly modeled. The fact that transmission in adjacent cells is, in general, not synchronized on a burst-by-burst basis will, in that case, be a major problem for multiuser detectors for two reasons.

- 1) Channel estimation must be performed for one user at a time, since the training sequences may not overlap. This will reduce the estimation accuracy, which leads to worse detection performance.

- 2) During the transmission of any single user, different users will interfere during different parts of the burst. When the interference scenario changes, the multiuser detector must be retuned.<sup>7</sup>

*Remark 2:* The considered system is sampled at the symbol rate. A single-input single-output system, where  $p$ -fold oversampling is employed, is in fact equivalent to a symbol-rate-sampled system with one input and  $p$  outputs. Hence, with oversampling, the dimension of the received signal vector increases with a factor equal to the oversampling factor. Oversampling is in this sense equivalent to multi-antenna receivers. However, excessive oversampling of a band-limited signal will lead to high correlation among consecutive samples, which in turn may lead to an ill-conditioned problem. Yet another way to increase the dimension of the received signal vector is described in [20]. This method is applicable only when the symbol constellation is one dimensional and doubles the effective number of antennas.

### B. Reducing the MIMO Model to Single-Input Multiple-Output (SIMO) Model with Colored Noise

If we explicitly model the signal from only one of the users, we have to consider signals from the remaining users as interference. Assuming the signal of interest to be signal number one, we define a disturbance vector  $V(k)$  as the sum of all CCI and noise

$$V(k) = \sum_{n=2}^M \mathbf{H}_n(z^{-1})s_n(k) + v(k) \quad (8)$$

where  $\mathbf{H}_n(z^{-1})$  is column  $n$  in (7). The interference  $V(k)$  is characterized by its matrix-valued covariance function

$$\bar{\psi}_{k-m} \triangleq E[V(k)V^H(m)]. \quad (9)$$

The complete SIMO channel model thus becomes

$$x(k) = \mathbf{H}_1(z^{-1})s_1(k) + V(k). \quad (10)$$

The DFE performing interference rejection will be based on this model.

*Remark 3:* If the model (10) is used as a basis for detector design, estimation of the matrix-valued covariance function (9) is vital. This becomes a major problem, since direct estimation of  $\bar{\psi}_m$  will provide poor accuracy for the short training sequences typically present in cellular systems. In fact, the estimates of the covariance function will be so unreliable that we, in Sections IV-B and V, are forced to exploit only the spatial structure of  $V(k)$ , i.e., we will assume that  $E[V(k)V^H(m)] = 0$  for  $k \neq m$ .

## III. THE MULTIVARIABLE DFE

### A. Design Equations

We shall use a multivariable DFE with a transversal feedforward filter and a transversal feedback filter

$$\begin{aligned} \hat{s}(k-\ell|k) &= \mathbf{S}(z^{-1})x(k) - \mathbf{Q}(z^{-1})\tilde{s}(k-\ell-1) \\ \tilde{s}(k-\ell) &= f(\hat{s}(k-\ell|k)). \end{aligned} \quad (11)$$

<sup>7</sup>In fact, this is a problem also for interference rejection (see [19]).

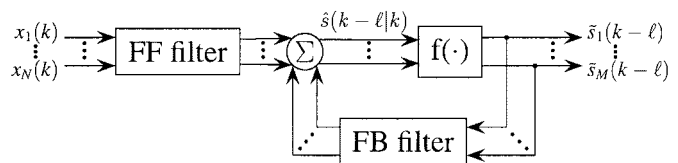


Fig. 2. The structure of the multivariable DFE, which exploits  $N$  sensor signals  $x_i(k)$  to compute estimates  $\tilde{s}(k-\ell)$  of symbols from  $M$  users. The feedforward filter and the feedback filter are both causal and of finite-order. A set of MISO DFE's can be represented in the same way but with a diagonal feedback filter.

Here,  $x(k)$  is the output of the array used as input to the equalizer, and  $\tilde{s}(k-\ell-1)$  are the decisions previously made by the equalizer. The soft estimate  $\hat{s}(k-\ell|k)$  is passed through the decision nonlinearity  $f(\cdot)$  to produce the hard estimate  $\tilde{s}(k-\ell)$ . The feedforward filter  $\mathbf{S}(z^{-1})$  is of order  $n_s$  with  $N$  inputs and  $M$  outputs, whereas the feedback filter  $\mathbf{Q}(z^{-1})$  is of order  $n_Q$  and has  $M$  inputs and  $M$  outputs. Note that the feedforward filter is causal and the decisions on the symbol vectors are made after a finite decision delay  $\ell$ . This means that the DFE is always realizable, in contrast to the DFE's presented in [4] and [18]. The MIMO DFE is depicted in Fig. 2.

The use of finite-impulse response filters in (11) and the use of model-based (indirect) design of the equalizer is motivated in [21].

To make derivation of optimal equalizer coefficients feasible, we adopt the common assumption that all previous decisions affecting the current symbol estimate are *correct*, i.e.,

$$\tilde{s}(k-\ell-n) = s(k-\ell-n), \quad n = 1, \dots, n_Q + 1. \quad (12)$$

Optimal coefficients of the DFE can then be computed from known channel and noise statistics.

Two criteria can be used for the determination of the coefficients of the filters  $\mathbf{S}(z^{-1})$  and  $\mathbf{Q}(z^{-1})$ : the peak distortion criterion and the minimum-mean square-error (MMSE) criterion.

1) *Zero-Forcing (ZF) Design:* A scalar equalizer derived by minimizing the peak distortion criterion minimizes the residual ISI. A scalar equalizer which removes all ISI is called a ZF equalizer. A natural multiuser extension to the peak distortion criterion is to minimize the residual ISI and CCI [4], and a multiuser ZF equalizer can be defined accordingly.

*Definition 1:* Consider the channel model (6) and a multivariable equalizer which forms the estimate  $\hat{s}(k-\ell|k)$  of a transmitted symbol vector  $s(k-\ell)$ . If

$$\hat{s}(k-\ell|k) = s(k-\ell) + \varepsilon(k) \quad (13)$$

where  $\varepsilon(k)$  is uncorrelated with all transmitted symbol vectors  $s(m) \forall m$ , then the equalizer is said to be ZF.

By substituting (5) and (12) into (11), the ZF condition (13) is seen to imply the relation

$$\mathbf{S}(z^{-1})\mathbf{H}(z^{-1})s(k) - \mathbf{Q}(z^{-1})s(k-\ell-1) = s(k-\ell).$$

A DFE will thus be ZF if and only if  $\mathbf{S}(z^{-1})$  and  $\mathbf{Q}(z^{-1})$  constitute a solution to the polynomial matrix, or Diophantine,

equation [22]

$$\mathbf{S}(z^{-1})\mathbf{H}(z^{-1}) - z^{-\ell-1}\mathbf{Q}(z^{-1}) = z^{-\ell}\mathbf{I}_M. \quad (14)$$

2) *MMSE Design*: The coefficients of a MMSE equalizer are determined to minimize

$$J = E[|s(k-\ell) - \hat{s}(k-\ell|k)|^2] \quad (15)$$

where the expectation is taken over the signal vector  $s(k)$  and the noise vector  $v(k)$ , defined in (3b) and (3c), respectively.

Under conditions which will be discussed in Section III-C, the MMSE DFE reduces to the ZF DFE when the covariance matrix of the noise  $v(k)$  in (6) goes to zero. In the following, we shall focus on the MMSE criterion, since the performance of a MMSE DFE is superior to that of a ZF DFE.

The matrix coefficients of the MMSE optimal multivariable DFE can be calculated as follows.

*Theorem 1*: Consider the multivariable DFE described by (11), the channel model (6) with  $M$  transmitters and  $N$  sensors, and the noise statistics (4) with  $\psi_0$  being nonsingular. Assume all  $M$  signals  $s_j(k)$  to be white with unit variance, mutually uncorrelated, and uncorrelated with the noise vector  $v(k)$ . If all past decisions are assumed correct, then the unique matrix polynomials  $\mathbf{S}(z^{-1})$  and  $\mathbf{Q}(z^{-1})$  in (11) of orders  $n_s$  and  $n_Q = L + n_s - \ell - 1$ , respectively, minimizing the MSE (15), are obtained as follows.

- 1) The feedforward filter  $\mathbf{S}(z^{-1}) = \mathbf{S}_0 + \mathbf{S}_1 z^{-1} + \dots + \mathbf{S}_{n_s} z^{-n_s}$  is determined by solving the system of  $N(n_s + 1)$  linear equations

$$(\mathcal{F}\mathcal{F}^H + \Psi) \begin{pmatrix} \mathbf{S}_0^H \\ \vdots \\ \mathbf{S}_{n_s}^H \end{pmatrix} = \begin{pmatrix} \mathbf{H}_\ell \\ \vdots \\ \mathbf{H}_0 \\ \mathbf{0} \end{pmatrix} \quad (16)$$

where  $\mathcal{F}$  is the  $N(n_s + 1) \times M(\ell + 1)$  matrix

$$\mathcal{F} \triangleq \begin{pmatrix} \mathbf{H}_0 & \dots & \mathbf{H}_\ell \\ \vdots & \ddots & \vdots \\ \mathbf{0} & \dots & \mathbf{H}_0 \\ \mathbf{0} & \dots & \mathbf{0} \end{pmatrix} \quad (17)$$

and where

$$\Psi = \begin{pmatrix} \psi_0 & \dots & \psi_{n_s} \\ \vdots & \ddots & \vdots \\ \psi_{-n_s} & \dots & \psi_0 \end{pmatrix}. \quad (18)$$

- 2) The coefficients of the feedback filter  $\mathbf{Q}(z^{-1}) = \mathbf{Q}_0 + \mathbf{Q}_1 z^{-1} + \dots + \mathbf{Q}_{n_Q} z^{-n_Q}$  are given by

$$\mathbf{Q}_n = \sum_{m=\max(0, n-L+\ell+1)}^{\min(n_s, \ell+n+1)} \mathbf{S}_m \mathbf{H}_{\ell+1-m+n} \quad (19)$$

where  $n_Q = L + n_s - \ell - 1$ .

*Proof*: See the Appendix.  $\blacksquare$

*Remark 1*: To compute a set of MMSE MISO DFE's, we use Theorem 1 repeatedly for each user of interest, with  $M = 1$  and with the noise statistic  $\bar{\psi}_n$  described by (9), substituted for  $\psi_n$ .

*Remark 2*: For a given detection scenario, the structure of the DFE is determined by the degrees of the feedforward and feedback filters as well as the decision delay. The impact of these three variables is outlined below.

- The degree  $n_s$  of the feedforward filter should be chosen to be as large as possible, at least equal to the decision delay  $\ell$ . When the noise is assumed to be temporally white ( $\psi_n = 0, n \neq 0$ ), (16) will give  $\mathbf{S}_n = 0$  for  $n > \ell$ . This is, however, *not* true when the noise is temporally colored, and choosing a feedforward filter degree which is larger than the decision delay can in this case give better performance.
- The degree  $n_Q$  of the feedback filter should be large enough to cancel all postcursor taps (taps with delay  $> \ell$ ) in the linearly equalized channel  $\mathbf{S}(z^{-1})\mathbf{H}(z^{-1})$ . The number of postcursor taps equals  $L + n_s - \ell$ , so we conclude that  $n_Q = L + n_s - \ell - 1$ .
- The decision delay  $\ell$  is chosen as a tradeoff between complexity and performance: the larger the decision delay, the better the performance. However, choosing  $\ell$  larger than the delay spread  $L$  only leads to minor improvements in performance.

*Remark 3*: In most DFE derivations (see, e.g., [4], [18], [23]), the following structure is assumed.

- A noncausal continuous-time filter matched to the received signal, followed by a symbol rate sampler, is used as a front end to the DFE.
- The discrete-time DFE, which operates on the sampled matched filter outputs, has feedforward and feedback filters with infinite impulse responses.

The derivation is based on the channel transfer function, and the resulting DFE is optimum when the decision delay is infinite. In contrast, the DFE obtained from Theorem 1 is a multivariable generalization of Mosen's adaptive feedback receiver [24]. The structure of the DFE is fixed, with finite impulse response (FIR) filters of predetermined degrees in both feedforward and feedback links. This structure is by no means optimal. However, for a DFE having this structure, Theorem 1 gives the optimal choice of the equalizer coefficients.

## B. Complexity

To compute the MMSE MIMO or MISO DFE, we need to solve the system of linear equations (16) and determine the feedback filter via (19). The number of required complex multiplications is indicated in Table I for both MIMO and MISO DFE's.

From Table I, we see that the complexity of a set of MISO DFE's is clearly comparable to a MIMO DFE for a realistic number of transmitters  $M$ . All differences in complexity arise from the different feedback filters. Both the feedback filter adjustment and the feedback filter operation is more complex for one MIMO DFE than for  $M$  MISO DFE's. However, in a DFE, the major complexity resides in the feedforward filter. First, to compute the coefficients of the feedforward filter, we need to solve a system of linear equations. Second, the feedforward filter must be implemented with multipliers,

TABLE I

NUMBER OF COMPLEX MULTIPLICATIONS NECESSARY TO COMPUTE AND RUN THE MIMO DFE AND A SET OF  $M$  MISO DFE'S FOR  $M$  USERS AND  $N$  SENSORS. DECISION DELAY OF THE DFE'S IS  $\ell$ , THE DEGREE OF THE FEEDFORWARD FILTER IS  $n_s$ , AND THE DELAY SPREAD IS  $L$ . DEGREE OF THE FEEDBACK FILTER IS  $n_Q = L + n_s - \ell - 1$

	MIMO DFE	MISO DFE
For the feedforward filter $S(z^{-1})$ :		
Calculate $\mathcal{F}\mathcal{F}^H + \Psi$		$\frac{1}{4}N^2M(\ell+1)(\ell+2)$
Factorize $\mathcal{F}\mathcal{F}^H + \Psi$		$\frac{1}{8}N^3(n_s+1)^3$
Solve for the filter coefficients		$N^2(n_s+1)^2M$
For the feedback filter $Q(z^{-1})$ :		
Compute the filter coefficients	$M^2N(L+1)(n_Q+1)$	$MN(L+1)(n_Q+1)$
Equalization of one symbol vector:		
Feedforward filtering		$MN(n_s+1)$
Feedback filtering	$M^2(n_Q+1)$	$M(n_Q+1)$

whereas the feedback filter typically can be implemented using only adders.

### C. Near-Far Resistance, Well-Posedness, and ZF Solutions

A MMSE DFE balances suppression of ISI and CCI against noise amplification. When the power of the interfering users is large, rejection of these strong signals is of paramount importance, whereas suppression of the noise is less important.

This situation has been studied extensively for CDMA multiuser detectors, in which case the ability to cope with strong interferers differs among detectors. If a CDMA multiuser detector is able to handle the detection of weak signals (often originating far from the receiver) in the presence of strong (near) interferers, the detector is said to be *near-far resistant* [25].

We may then ask under what conditions are MIMO and MISO DFE's near-far resistant? To investigate this question, we let the noise covariance  $\psi_n$  tend to zero in (4) [and (9)]. If all ISI and CCI can be removed, the MMSE equalizer will reduce to a ZF equalizer, and the estimation error will vanish. In this case, perfect equalization is possible for *any* power of the interfering users. If no ZF equalizer exists, all ISI and CCI cannot be removed, so the estimation error will not vanish.

When a ZF solution exists, good performance can be achieved when the signal-to-noise ratio (SNR) goes to infinity. The consequences of this fact must, however, be interpreted with some care. When the ZF problem is in some sense well-conditioned, the corresponding MMSE equalizer will work well also at realistic SNR's. However, when the ZF problem is ill-conditioned,<sup>8</sup> the corresponding MMSE solution may not provide adequate performance, despite the fact that a ZF solution does exist. We believe, however, that the likelihood for this situation to occur is small.

We can therefore use the existence of a ZF DFE as a proof of near-far resistance for the MMSE MIMO DFE or the MMSE MISO DFE. In more general terms, the existence of a ZF solution also indicates that the equalization problem is well posed in the sense that it can provide a useful solution: good performance can be guaranteed, if the noise level is sufficiently low.

<sup>8</sup>This would occur, for instance, if the channels of different users were almost identical.

A solution to the ZF equation (14) exists if and only if [22]

$$\text{Every common right divisor of } \mathbf{H}(z^{-1}) \text{ and } z^{-\ell-1}\mathbf{I}_M \text{ is also a right divisor of } z^{-\ell}\mathbf{I}_M. \quad (20)$$

If (20) is fulfilled, we know that a ZF solution exists. However, it remains to specify the filter degrees of such DFE's. This is the topic of Theorem 2.

As a prerequisite, we need the following definitions. We first factorize  $\mathbf{H}(z^{-1})$  into three matrix polynomials

$$\mathbf{H}(z^{-1}) = \overline{\mathbf{H}}(z^{-1})\mathbf{G}(z^{-1})\mathbf{D}(z^{-1}). \quad (21)$$

The factors of (21) are defined as

$$\mathbf{D}(z^{-1}) \triangleq \text{diag}(z^{-d_1} \quad \dots \quad z^{-d_M}) \quad (22a)$$

$$\mathbf{G}(z^{-1}) \triangleq \text{diag}(G_1(z^{-1}) \quad \dots \quad G_M(z^{-1})) \quad (22b)$$

$$\overline{\mathbf{H}}(z^{-1}) \triangleq \overline{\mathbf{H}}_0 + \overline{\mathbf{H}}_1 z^{-1} + \dots + \overline{\mathbf{H}}_L z^{-L} \quad (22c)$$

where

$$d_j \triangleq \text{the propagation delay for user } j, d_j \leq \ell \quad (23a)$$

$$G_j(z^{-1}) \triangleq \text{the greatest common polynomial factor}^9 \text{ of the channels } H_{1j}(z^{-1}), \dots, H_{Nj}(z^{-1}) \text{ from user } j \text{ to all antenna elements.} \quad (23b)$$

We also define

$$g_j \triangleq \text{deg } G_j(z^{-1}) \quad (24a)$$

$$\overline{L}_j \triangleq \max_i L_{ij} - d_j - g_j. \quad (24b)$$

We are now ready to formulate Theorem 2.

*Theorem 2:* Consider the MIMO channel model (6) with  $M$  sources and  $N$  sensors with  $M \leq N$  and assume that (20) holds. A generically necessary<sup>10</sup> condition for the existence of a ZF MIMO DFE (11) with decision delay  $\ell$  and feedforward filter degree  $n_s$  is then

$$n_s \geq \frac{M(\ell+1) - \sum_{m=1}^M d_m}{N} - 1. \quad (25)$$

The condition

$$n_s \geq \max_j \frac{\sum_{m=1}^M \overline{L}_m + \ell + 1 - \overline{L}_j - d_j}{N + 1 - M} - 1 \quad (26)$$

is generically necessary for existence of a set of MISO DFE's with decision delay  $\ell$  and feedforward filter degree  $n_s$ .

<sup>9</sup>Such a common factor could be caused by, e.g., the pulse shaping function.

<sup>10</sup>Generic necessity of the degree conditions in Theorem 2 should be understood in the sense that when these claims are violated, a ZF equalizer exists with probability zero if the channel taps  $\mathbf{H}_0, \dots, \mathbf{H}_L$  are random matrices with independent elements.

*Proof:* See [21].<sup>11</sup> ■

When either the condition (25) or the condition (26) is violated, the corresponding detector will not have enough degrees of freedom to completely cancel all the interfering rays which impinge on the array.

*Remark 4:* To some extent, oversampling can be used to effectively increase the number of antennas, as mentioned in Section II-A. Also, when the symbol constellation is one-dimensional, the conditions above can be somewhat relaxed.

*Remark 5:* If either the condition (20) or the degree condition (25) or (26) is not satisfied, then the corresponding MMSE detector will not work as intended when the signal levels for the interfering users are large. However, the effects of the nonexistence of a ZF equalizer will be visible already for moderate SNR's, since the residual CCI will cause bit errors at all noise levels.

The impact of a violation of the inequality (26) will be demonstrated in Section IV-A.3.

#### IV. MONTE CARLO SIMULATIONS

To explore the performance of the MIMO DFE as a tool for joint multiuser detection, extensive simulation experiments are conducted. The experiments are designed to illustrate several key aspects of a real-world implementation of a system employing reuse within a cell. We also compare the performance of the MIMO DFE (multiuser detection) with the performance of the MISO DFE (interference rejection).

Some of the simulation scenarios correspond to both uplink and downlink situations. In a few of the scenarios, specific uplink issues are investigated.

In our scenario, one, two, three, or four BPSK modulated signals impinge on an antenna array with four antenna elements. Each signal has passed through a frequency-selective three-tap channel. Each tap is time-invariant over the duration of a TDMA burst, but subject to Rayleigh fading between bursts. Different taps in the channel fade independently.<sup>12</sup> The channels from different transmitters to one receiver antenna are mutually uncorrelated. The signals are received in the presence of additive Gaussian noise, which is both temporally and spatially white. The smoothing lags and feedforward filter lengths of both DFE's are chosen equal to the length to the channel impulse response ( $\ell = n_s = L = 2$ ).

In different simulations, the system specified above is investigated under the following additional conditions.

- Known channels (Section IV-A) with:
  - a) equal average SNR of all users and uncorrelated antennas;
  - b) equal average SNR of all users and correlated antennas; and
  - c) different average SNR of the users and uncorrelated antennas.

<sup>11</sup> [Online]. Available HTTP://www.signal.uu.se/Publications/abstracts/r981.html

<sup>12</sup> We thus assume uncorrelated scattering [23] and neglect the impact of the pulse shaping. In practice, the pulse shaping will introduce some correlation among adjacent taps, but with full-response signaling, this correlation is small and will not affect the results in the simulations.

- Estimated channels (Section IV-B):
  - a) estimation using the training sequence only;
  - b) estimation using detected data, with a so-called *bootstrap* method [26].

##### A. Known Channel Coefficients and Noise Covariances

In this section, we shall study the idealized case when all channel coefficients are exactly known. Effects caused by differences in detector structure can be studied here in isolation, since effects of channel estimation errors are avoided.

1) *Equal Average SNR for all Users and Uncorrelated Antennas:* This is the basic scenario, where all users have the same average SNR, and the channels from a single transmitter to different antenna elements are uncorrelated. In practice, the condition of all users having the same average SNR can be fulfilled by using slow power control, which compensates for the propagation loss and the shadow fading. The condition of uncorrelated antennas presupposes a sufficiently large antenna spacing at the base station. For downlink transmission, the antennas at the mobile must also be placed sufficiently far apart, although the required spacing is much smaller than at the base station.

The above scenario is simulated for an average SNR per bit between 0 and 15 dB, where the average SNR per bit [23] for user  $j$ ,  $\bar{\gamma}_b^j$ , is defined as

$$\bar{\gamma}_b^j = \frac{1}{N} \frac{E[|H_{ij}^0|^2 + |H_{ij}^1|^2 + |H_{ij}^2|^2] E[|s_j(k)|^2]}{E[|v_i(k)|^2]} \quad (27)$$

where we have divided by  $N$  to enable a fair comparison between scenarios with different number of antenna elements.<sup>13</sup> We assume that  $\bar{\gamma}_b^j$  is equal at different antenna elements and thus independent of  $i$ .

Fig. 3 shows the estimated BER as a function of the average SNR per bit. With four users, the performance of the MIMO DFE at  $\bar{\gamma}_b^j = 15$  dB is around 6 dB better than the performance of the MISO DFE. This difference arises from the fact that the MISO DFE uses up all its degrees of freedom to cancel the interference from the other users. This task is easier for the MIMO DFE since its feedback filter takes care of some of the suppression of the cochannel interferers. For fewer users, the difference between the two approaches is smaller. See Table II for a performance summary.

2) *Equal Average SNR for all Users and Correlated Antennas:* In a realistic uplink scenario with phased array receivers, the channels from a single user to the different antenna elements will be correlated. However, successful multiuser detection does not require uncorrelated antennas. With perfectly correlated antennas, the antenna array can form narrow beams, which enhance the desired signal and suppress interference, arriving from other directions.

In this simulation, we will assume that a uniform linear array is present at the base station. The mobile is assumed

<sup>13</sup> Thus, we do *not* use the SNR per channel, defined as  $\bar{\gamma}_c^j \triangleq N\bar{\gamma}_b^j$ . Also note that signals from other users do *not* affect  $\bar{\gamma}_b^j$ . Adding users will instead increase the resulting bit-error rate (BER) for a fixed  $\bar{\gamma}_b^j$  and thereby demonstrate the performance degradation as a function of the system load.

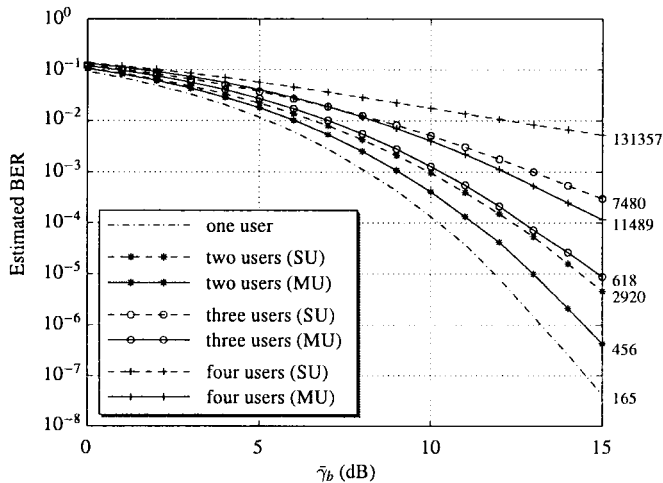


Fig. 3. Comparison of the MIMO DFE (MU) and the MISO DFE (SU) for known channels, equal transmitter powers, and uncorrelated antennas. The numbers to the right of the graph are the number of errors used to estimate the BER for the average SNR per bit  $\bar{\gamma}_b = 15$  dB.

TABLE II

PERFORMANCE LOSS EXPERIENCED WHEN ADDING USERS AS COMPARED TO A SINGLE-USER SYSTEM FOR THE SIMULATION SCENARIOS IN SECTIONS IV-A.1, IV-B.1, AND IV-B.2. ALL VALUES ARE ESTIMATED AT AN SNR OF 15 dB

Number of users	MISO			MIMO		
	2	3	4	2	3	4
Known channels	2.6 dB	5.6 dB	8.9 dB	1.2 dB	3.0 dB	5.0 dB
Estimated channels using the training sequence only	6.0 dB	10.5 dB	12.9 dB	1.8 dB	4.2 dB	7.3 dB
the two pass algorithm	5.9 dB	11.2 dB	14.0 dB	1.5 dB	3.3 dB	5.6 dB

to be located inside a cluster of scatterers, which act as secondary transmitters. The shape of the cluster determines the actual antenna correlation, but different shapes give similar results [27]. We will assume a circular scatterer distribution. For this scenario, Fulghum *et al.* [28] obtained the following approximation for the antenna correlation

$$\rho(\delta, R, r, \theta) = J_0\left(\frac{2\pi\delta R}{r} \cos\theta\right) e^{-j2\pi\delta \sin\theta} \quad (28)$$

where

- $\delta$  antenna separation, expressed in carrier wavelengths;
- $R$  antenna separation, expressed in carrier wavelengths;
- $r$  distance between the receiver and the transmitter;
- $\theta$  angle of the incoming signal with respect to antenna broadside;

and where  $J_0$  is the Bessel function of the first kind and order zero. To model the frequency selective fading, we use the model proposed in [27]. In this model, each vector tap in the impulse response will be associated with a separate cluster of secondary transmitters. The angular locations  $\theta$  of scatterer distributions corresponding to different column vector taps in the impulse response are assumed to be independent stochastic variables, uniformly distributed in the interval  $[-90^\circ, 90^\circ]$ .

The antenna correlations according to (28) will depend on the angles  $\theta$ , which are not under the system designer's control. Therefore, we shall address the performance of the DFE as a function of the correlation coefficient according to (28) that

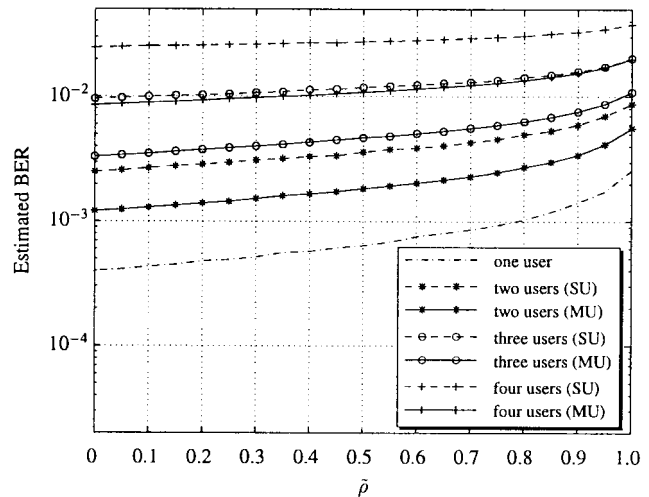


Fig. 4. Comparison of the MIMO DFE (MU) and the MISO DFE (SU) for a uniform linear array with *correlated antenna elements*. The channels are known and the SNR per bit is  $\bar{\gamma}_b = 10$  dB for all users. The estimated BER is shown as a function of the antenna correlation  $\tilde{\rho}$  that would result if all signals were impinging at an angle of  $\theta = 0^\circ$ .

would result if the signals would all impinge from an angle  $\theta = 0^\circ$

$$\rho(\delta, R, r, \theta = 0) = J_0\left(\frac{2\pi\delta R}{r}\right) \triangleq \tilde{\rho}\left(\frac{\delta R}{r}\right). \quad (29)$$

The quantity  $\tilde{\rho}$  can be measured for a given environment and array, and the corresponding performance can be predicted from the simulation results presented below.

The simulation results are presented in Fig. 4 for an SNR of 10 dB and antenna correlations between zero and one.

It is evident from Fig. 4 that successful multiuser detection and interference rejection are indeed not dependent on uncorrelated antennas. The performance of all algorithms deteriorates when the antenna correlation is increased from zero to one. This is due to the diminished diversity effect, resulting from a decrease in the number of diversity branches. However, the multiuser detection approach retains its superior performance as compared to the interference rejection approach.

*Remark 1:* Notice that  $\tilde{\rho} = 0$  does *not* imply that all channel taps are uncorrelated, only that a signal that impinges from  $\theta = 0^\circ$  would result in uncorrelated taps. Therefore, the BER for  $\tilde{\rho} = 0$  does not coincide with the BER for  $\bar{\gamma}_b = 10$  dB in Fig. 3, where *all* taps are uncorrelated.

*Remark 2:* Of course, antenna correlation also affects the performance of the proposed downlink scheme. This is investigated in [16], and the results for a multiuser detector operating in the downlink are very similar to the uplink case investigated here.

3) *Different Average SNR for the Users and Uncorrelated Antennas:* In Sections IV-A.1 and IV-A.2, we assumed that power control was used to compensate for the propagation loss and the shadow fading. In the scenario investigated in this section, we will relax this assumption: even the average received powers will differ among the users. This will generate the so-called *near-far problem*.

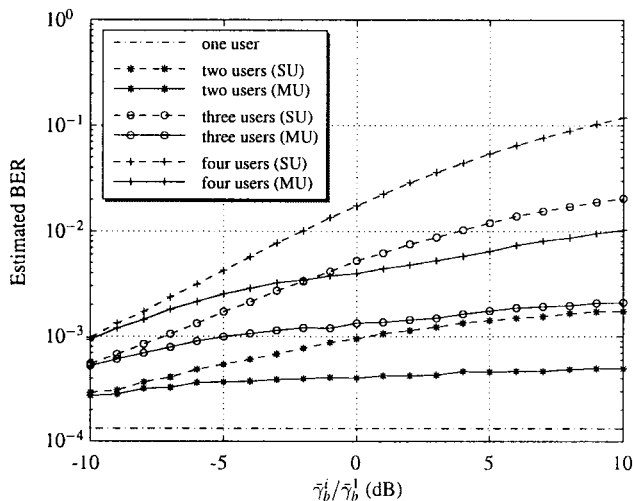


Fig. 5. Comparison of the MIMO DFE (MU) and the MISO DFE (SU) for known channels, different transmitter powers, and uncorrelated antennas. In this simulation, 25 000 channels were randomly selected. Over each channel, 1000 symbols were transmitted. User number one has an SNR per bit of  $\bar{\gamma}_b^1 = 10$  dB, while the SNR per bit  $\bar{\gamma}_b^i$  of the other users is equal and varies.

We estimated the BER of a user having an average SNR per bit of 10 dB in a scenario where there are one, two, or three additional users, each having an average SNR per bit that is between 0 and 10 dB higher, i.e., between 10 and 20 dB. The result from this simulation is depicted in the right half of Fig. 5.

In a MIMO DFE, decisions concerning one user affect future symbol estimates of all users. Incorrect decisions on the symbols from a weak user will thus impair the decisions of other stronger users. In this case, a MISO DFE may yield better performance since (possibly incorrect) decisions of the weaker users' symbols do not influence the estimates of the stronger users' symbols.

To investigate this effect, we estimate the BER of a user having an average SNR per bit of 10 dB in a scenario where there were one, two, or three additional users, each having an average SNR per bit which was between 0 and 10 dB lower, i.e., the SNR per bit of the remaining users varied between 10 and 0 dB. The result from this simulation is depicted in the left half of Fig. 5.

From the leftmost part of Fig. 5, it is clear that for the investigated differences in power levels, error propagation is not so severe that the BER of a MIMO DFE exceeds the BER of a MISO DFE. On the other hand, from the rightmost part of Fig. 5, it is evident that for the MIMO DFE, four users can coexist in the cell, even when the received average powers differ substantially. However, the performance of the MISO DFE is seriously affected by the increase of the power levels of the interfering users, since this MISO DFE does not comply with the ZF condition (26). Inserting numerical values into (26), we find that complete suppression of all cochannel interferers is impossible whenever  $M \geq 3$ . As the transmitter powers of these users increase, the estimation error due to residual interference increases, resulting in an increased BER. The MIMO DFE on the other hand is capable of completely removing the interference from the stronger users, at the expense of a slightly increased noise amplification.

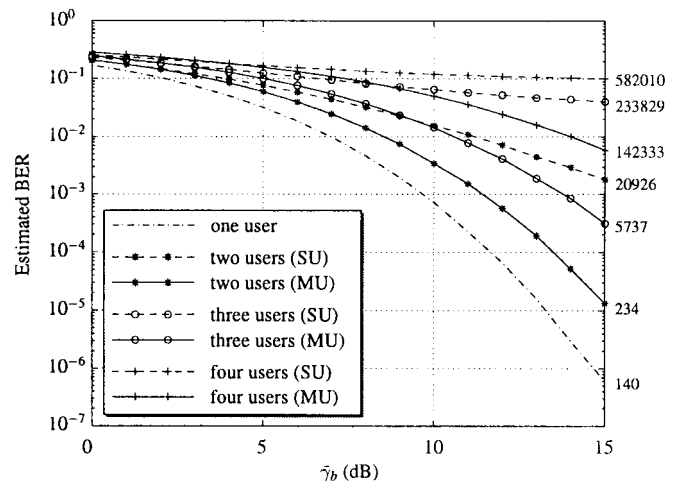


Fig. 6. Comparison of the MIMO DFE (MU) and the MISO DFE (SU) for estimated channels, equal transmitter powers, and uncorrelated antennas. The channel was estimated using only the training sequence. The numbers at the right edge of the graph are the number of errors used to estimate the BER for an SNR per bit of  $\bar{\gamma}_b = 15$  dB.

## B. Estimated Channel Coefficients

1) *Estimation Using the Training Sequence Only:* To demonstrate how the MIMO DFE works in a more realistic case, channel estimation is introduced. The data is transmitted in bursts with a structure similar to that of GSM. A training sequence of 26 symbols is located in the middle of each burst. Together with data symbols, tail symbols, and control symbols, this results in a total burst length of 148 symbols.<sup>14</sup> The channel estimation is performed using the offline least squares method, and the spatial color of the noise is estimated from the residuals of the channel identification. The temporal color of the noise is not estimated due to the limited amount of data. Apart from this, the simulation conditions are the same as in Section IV-A.1. The results are indicated in Fig. 6.

When we compare Figs. 3 and 6, we see that the difference between the MIMO DFE and the MISO DFE is greater when the channels have to be estimated. The inability to estimate and, subsequently, use the temporal color of the interference leads to a large performance degradation for interference rejection. Again, the difference in performance is larger when more users are active in the system. Table II summarizes the performance loss of the MISO DFE and the MIMO DFE for known and estimated channels as compared to the single-user case.

2) *Improving Channel Estimation Using the Detected Symbols:* Since channel estimation errors are a major cause of bit errors in a digital cellular system, there is a great potential for performance improvement in the reduction of the channel estimation errors. One way of accomplishing this would be to use detected symbols as regressors in the estimation algorithm. By using these extra regressors, we can increase the length of the training sequence from 26 to 148 symbols in the GSM case. This *bootstrap* method is based on the assumption that when the fraction of incorrect decisions from pass one is sufficiently small, the channel estimation in pass two will provide better

<sup>14</sup>The pulse shaping used in GSM results in a channel with five highly correlated taps. We have not included this feature in the simulation. Only the burst structure resembles the one used in GSM.

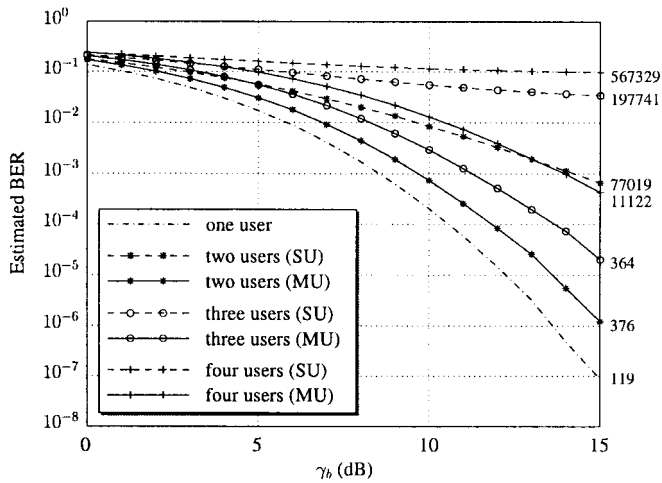


Fig. 7. Comparison of the MIMO DFE (MU) and the MISO DFE (SU) for estimated channels, equal transmitter powers, and uncorrelated antennas. The channel estimates were obtained using *both the training sequence and detected symbols*. The numbers at the right edge of the graph are the number of errors used to estimate the BER for an SNR per bit of  $\bar{\gamma}_b = 15$  dB.

accuracy than the channel estimation in pass one. Bootstrap equalization is discussed in [26] for both DFE's and MLSE.

To test this algorithm, we repeat the simulation in Section IV-B.1 with the use of the detected symbols to improve the channel estimates, according to the bootstrap algorithm described above. The results from the second pass of the algorithm are shown in Fig. 7.

As can be seen from Fig. 7, the BER was reduced when the tentative decisions were used to improve the channel estimates. It seems that the performance of the multiuser detector was impaired more by the poor quality of the channel estimates than the performance of the detector performing interference rejection. The difference between the two approaches is larger when the two-pass algorithm is used than when only the training sequence is used to estimate the channel. This is due to the fact that the estimation of the covariance function of the noise and the interference is still inaccurate, despite the fact that we now have access to a training sequence of 148 symbols.

The performance at 15 dB of the bootstrap algorithm is summarized in Table II.

## V. APPLICATION ON EXPERIMENTAL DATA

The simulations in Section IV indicate that reuse within a cell is indeed possible. But will it work in practice? To investigate this, we will apply the methods described in Section III to a set of uplink measurements.

### A. Measurements

The measurements were performed on a testbed constructed by Ericsson Radio Systems AB and Ericsson Microwave Systems AB [29]. The testbed implements the air interface of a DCS-1800 base station, and the measurements were performed in Kista, a suburb of Stockholm, Sweden.

The array consists of four antenna elements, each having two polarization diversity branches, resulting in eight antenna outputs. A conventional sector antenna with two-branch polarization diversity is also included in the measurement setup

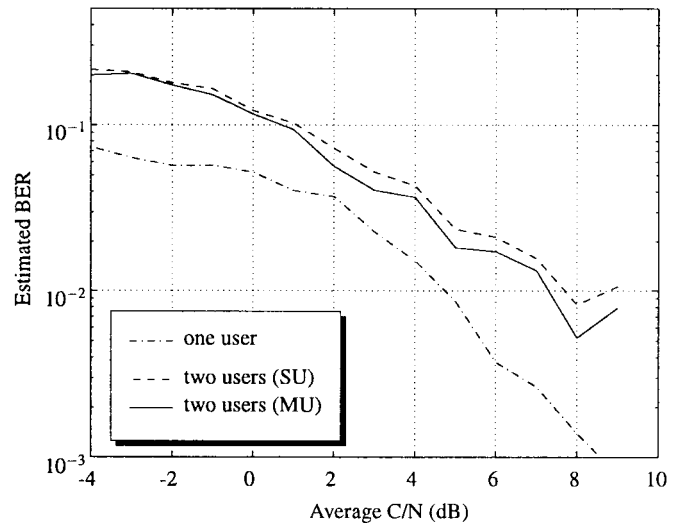


Fig. 8. Comparison of the MIMO DFE (MU) and the MISO DFE (SU) applied to uplink measurements from a DCS-1800 testbed. The receive antenna had eight outputs and two users were transmitting simultaneously.

for two reasons: to evaluate the impact of using more antenna elements and to estimate the transmitted signal power.

A single mobile mounted in a van was used for all experiments. The mobile transmitted GSM bursts, which were received, sampled, and recorded, both for the sector and the array antenna. Two sets of measurements were collected and added to represent a situation when two mobile users share the same channel. The algorithms investigated in Section IV were then applied to the recorded data.

The performance of the DFE's was evaluated as a function of the average *carrier-to-noise ratio* (C/N).<sup>15</sup> This quantity cannot be directly measured. Instead, it was estimated indirectly. For details, see [21].

### B. Results

The frame structure in DCS-1800 is identical to the one described in Section IV-B. In this case, five tap channels are estimated, and  $n_s = \ell = L = 4$  is used.

The MMSE MIMO DFE and two MMSE MISO DFE's were used to demodulate the signals from the two users. In both cases, the bootstrap algorithm described in Section IV-B.2 was utilized. The results are shown in Fig. 8 for the array antenna and in Fig. 9 for the sector antenna.

The results from the experiments on the measurements from the array antenna are not surprising. For the lightly loaded system with  $N = 8$  and  $M = 2$ , the performance of a MIMO DFE should be only slightly better than the performance of two MISO DFE's.

For the sector antenna, the results are more surprising: a MIMO DFE performs slightly *worse* than two MISO DFE's. The reason for this is twofold.

- 1) With the sector antenna, the channel is in fact flat fading. All ISI is caused by the partial-response modulation, and the same frequency selective fading is experienced

<sup>15</sup>The C/N corresponds to the SNR per channel discussed previously. We use the notation C/N rather than SNR to stress the fact that the quantity has been estimated indirectly.

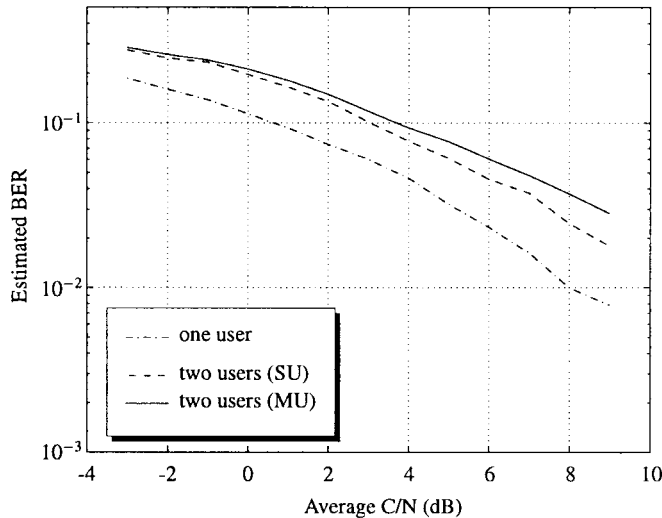


Fig. 9. Comparison of the MIMO DFE (MU) and the MISO DFE (SU) applied to uplink measurements from a DCS-1800 testbed. The receive antenna had two outputs and two users were transmitting simultaneously.

at different antenna elements. Hence, each column of  $\mathbf{H}(z^{-1})$  will have a common factor of degree  $L$ . For  $N = 2$  and  $M = 2$ , the ZF condition (26) then reduces to  $n_s \geq \ell - d_j$ , where  $\ell$  is the decision delay and  $d_j$  is the propagation delay of user  $j$ . Therefore, the choice  $n_s = \ell$  ensures the existence of a ZF MISO DFE for this scenario, and the corresponding MMSE detector will work well.

- 2) When all ISI is caused by the modulation, all rays impinge on the array from the same direction. In this case, spatial-only interference rejection is sufficient to suppress the interfering user. The MIMO DFE tries to reject the CCI by means of an estimate of its spatio-temporal color. This will lead here to *worse* performance, since parameters, which do not improve equalization, are estimated.

With the array antenna, a few multipath components can be resolved, which leads to a situation where the channels to different antenna elements will have no common factor. In this case, the interference canceller will have to place spatial nulls in several directions, thereby sacrificing some degrees of freedom, which leads to worse performance. In this case, the multiuser detector can use its additional degrees of freedom to cancel the CCI.

It should be noted that the investigated scenario constitutes a very difficult detection problem: the two mobiles travel exactly the same measurement route. Still, reuse within a cell is possible, using either the array antenna or the sector antenna: The detector performance is approximately 2 dB worse for two users than for one user.

## VI. DISCUSSION AND CONCLUSIONS

In our investigation of receiver algorithms designed to accomplish reuse within cells, we have compared MIMO DFE's which work as multiuser detectors to the use of interference rejection, implemented by MISO DFE's. Realizable MMSE equalizers of both kinds have been derived, based on channel models and noise spectral models.

In summary, extensive simulations indicate that channel reuse within a cell is indeed a viable option, with multiuser detection providing superior performance. Up to four users could coexist in the same cell if the receivers utilize antenna arrays with only four antenna elements. With multiuser detection, the price paid for this in increased BER is rather small. We have tested the algorithms on experimental measurements from a DCS-1800 testbed. For the investigated scenario, reuse within a cell is possible using either an eight-element antenna array or a two-branch diversity sector antenna.

Differences in performance between multiuser detection and interference rejection are partly due to the difference in detector *structure*: a multiuser (MIMO) DFE utilizes feedback from previously estimated symbols from *all* users, while the interference rejecting (MISO) DFE performs decision feedback from the user of interest only.

The difference also results from the preconditions for *channel estimation*. In the multiuser case, input-output transfer functions from each transmitter to each receiver antenna can and must be estimated. For interference rejection, the CCI constitutes colored noise, and multivariate noise models estimated from short data records will have poor accuracy.

These factors will in general result in a higher performance for the multiuser detector. This is particularly apparent when the detectors are applied to heavily loaded systems (with many users/interferers) and when the delay spread in the multipath channel is large.

Both multiuser detectors and interference rejecting MISO DFE's can be made near-far resistant. However, the conditions for this, as indicated by the existence of a ZF solution, are more restrictive when using interference rejection.

Our conclusions are based on studies and comparisons of symbol-by-symbol DFE's. We would expect similar conclusions to hold from a comparison of joint multiuser maximum-likelihood (ML) detectors [30] to single-user ML detectors with spatial interference whitening [6]. The results in [31] confirm this assumption. However, for ML detectors the complexity of the two approaches would differ substantially, in contrast to the complexity of the two detectors described here.

## APPENDIX

### DERIVATION OF THE MIMO MMSE DFE

Suppose that a linear time-invariant FIR channel of order  $L$  is given by (6) and assume that

$$\begin{aligned} E[s(k)s^H(m)] &= \delta_{km}I \\ E[v(k)v^H(m)] &= \psi_{k-m} \\ E[s(k)v^H(m)] &= 0. \end{aligned} \quad (30)$$

The objective is to estimate the symbol vector  $s(k - \ell)$ , by means of the *MIMO DFE* defined in (11), i.e.,

$$\hat{s}(k - \ell|k) = \mathbf{S}(z^{-1})x(k) - \mathbf{Q}(z^{-1})\tilde{s}(k - \ell - 1) \quad (31)$$

$$\begin{aligned} &= \sum_{n=0}^{n_s} \mathbf{S}_n x(k - n) - \sum_{m=\ell+1}^{L+n_s} \mathbf{Q}_{m-\ell-1} \tilde{s}(k - m) \\ &= \Theta_S^H x_k - \Theta_Q^H \tilde{s}_{k-\ell-1} \end{aligned} \quad (32)$$

$$\tilde{s}(k - \ell) = f(\hat{s}(k - \ell|k)). \quad (33)$$

Above, we have defined

$$\Theta_S^H \triangleq (\mathbf{S}_0 \ \mathbf{S}_1 \ \cdots \ \mathbf{S}_{n_s}) \quad (34a)$$

$$\Theta_Q^H \triangleq (\mathbf{Q}_0 \ \mathbf{Q}_1 \ \cdots \ \mathbf{Q}_{L+n_s-\ell-1}) \quad (34b)$$

and

$$x_k \triangleq (x^T(k) \ x^T(k-1) \ \cdots \ x^T(k-n_s))^T \quad (35a)$$

$$\tilde{s}_{k-\ell-1} \triangleq (\tilde{s}^T(k-\ell-1) \ \cdots \ \tilde{s}^T(k-n_s-L))^T. \quad (35b)$$

The coefficients  $\{\mathbf{S}_n\}$  and  $\{\mathbf{Q}_n\}$  are to be determined so that the MSE of the estimate  $\hat{s}(k-\ell|k)$  is minimized. The mean square of

$$\varepsilon(k-\ell) = s(k-\ell) - \hat{s}(k-\ell|k) \quad (36)$$

is minimized if the estimation error is orthogonal to all signals which the estimate  $\hat{s}(k-\ell|k)$  may be based upon, i.e.,  $x_k$  and  $\tilde{s}_{k-\ell-1}$ . The matrix filter coefficients providing the minimum mean-square estimation error are thus determined by the orthogonality condition

$$E \left[ \begin{pmatrix} x_k \\ -\tilde{s}_{k-\ell-1} \end{pmatrix} \varepsilon^H(k-\ell) \right] = 0. \quad (37)$$

If we insert  $\varepsilon(k-\ell)$  from (37) and  $\hat{s}(k-\ell|k)$  from (32), we obtain

$$\begin{pmatrix} E x_k x_k^H & -E x_k \tilde{s}_{k-\ell-1}^H \\ -E \tilde{s}_{k-\ell-1} x_k^H & E \tilde{s}_{k-\ell-1} \tilde{s}_{k-\ell-1}^H \end{pmatrix} \begin{pmatrix} \Theta_S \\ \Theta_Q \end{pmatrix} = \begin{pmatrix} E x_k s^H(k-\ell) \\ -E \tilde{s}_{k-\ell-1} s^H(k-\ell) \end{pmatrix}. \quad (38)$$

Assume that all previous decisions were correct, i.e.,  $\tilde{s}(k-n) = s(k-n)$ ,  $n = \ell+1, \dots, L+n_s$ , and define

$$s_{k-\ell-1} = (s^T(k-\ell-1) \ \cdots \ s^T(k-n_s-L))^T. \quad (39)$$

Due to the assumption of uncorrelated symbols made in (30), (38) can then be simplified to

$$\begin{pmatrix} E x_k x_k^H & -E x_k s_{k-\ell-1}^H \\ -E s_{k-\ell-1} x_k^H & I \end{pmatrix} \begin{pmatrix} \Theta_S \\ \Theta_Q \end{pmatrix} = \begin{pmatrix} E x_k s^H(k-\ell) \\ 0 \end{pmatrix}. \quad (40)$$

To evaluate the expectations in (40), we invoke the channel model (6) to obtain an explicit expression for  $x_k$

$$x_k = \begin{pmatrix} \mathbf{H}_0 & \cdots & \mathbf{H}_L & \cdots & 0 \\ \vdots & \ddots & & \ddots & \vdots \\ 0 & \cdots & \mathbf{H}_0 & \cdots & \mathbf{H}_L \end{pmatrix} \begin{pmatrix} s(k) \\ \vdots \\ s(k-n_s-L) \end{pmatrix} + \begin{pmatrix} v(k) \\ \vdots \\ v(k-n_s) \end{pmatrix}. \quad (41)$$

To obtain a more compact expression of (41), we introduce

$$v_k \triangleq (v^T(k) \ v^T(k-1) \ \cdots \ v^T(k-n_s))^T \quad (42a)$$

$$\bar{s}_k \triangleq (s^T(k) \ s^T(k-1) \ \cdots \ s^T(k-\ell+1))^T. \quad (42b)$$

Furthermore, we define the following matrices:

$$\mathcal{F}_{\text{tot}} \triangleq \left( \begin{array}{ccccc} \mathbf{H}_0 & \cdots & \mathbf{H}_L & \cdots & 0 \\ \vdots & \ddots & & \ddots & \vdots \\ 0 & \cdots & \mathbf{H}_0 & \cdots & \mathbf{H}_L \end{array} \right) \Bigg\}^{N(n_s+1)} \\ \triangleq (\mathcal{F}_{\text{fut}} \ \mathcal{F}_{\text{pres}} \ \mathcal{F}_{\text{past}}) \quad (43a)$$

where we have defined

$$\mathcal{F}_{\text{fut}} \triangleq \text{The first } M\ell \text{ columns in } \mathcal{F}_{\text{tot}} \quad (43b)$$

$$\mathcal{F}_{\text{pres}} \triangleq \text{Columns } M\ell+1 \text{ to } M(\ell+1) \text{ in } \mathcal{F}_{\text{tot}} \quad (43c)$$

$$\mathcal{F}_{\text{past}} \triangleq \text{Columns } M(\ell+1)+1 \text{ to } M(n_s+L+1) \text{ in } \mathcal{F}_{\text{tot}}. \quad (43d)$$

Equation (41) can then be written as

$$x_k = \mathcal{F}_{\text{fut}} \bar{s}_k + \mathcal{F}_{\text{pres}} s(k-\ell) + \mathcal{F}_{\text{past}} s_{k-\ell-1} + v_k \quad (44)$$

where  $s_{k-\ell-1}$  was defined in (39). Using (44) and (30), we can compute the expectations in (40) and insert them into the normal equations (40)

$$\begin{pmatrix} \mathcal{F}_{\text{fut}} \mathcal{F}_{\text{fut}}^H + \mathcal{F}_{\text{pres}} \mathcal{F}_{\text{pres}}^H + \mathcal{F}_{\text{past}} \mathcal{F}_{\text{past}}^H + \Psi & -\mathcal{F}_{\text{past}} \\ -\mathcal{F}_{\text{past}}^H & I \end{pmatrix} \cdot \begin{pmatrix} \Theta_S \\ \Theta_Q \end{pmatrix} = \begin{pmatrix} \mathcal{F}_{\text{pres}} \\ 0 \end{pmatrix} \quad (45)$$

where  $\Psi$  is given by (18). By observing that  $\Theta_Q = \mathcal{F}_{\text{past}}^H \Theta_S$  from the second block row of (45) and inserting this into the first block row, we obtain

$$(\mathcal{F}_{\text{fut}} \mathcal{F}_{\text{fut}}^H + \mathcal{F}_{\text{pres}} \mathcal{F}_{\text{pres}}^H + \Psi) \Theta_S = \mathcal{F}_{\text{pres}} \quad (46a)$$

$$\Theta_Q = \mathcal{F}_{\text{past}}^H \Theta_S. \quad (46b)$$

Now observe that  $(\mathcal{F}_{\text{fut}} \ \mathcal{F}_{\text{pres}}) = \mathcal{F}$  as defined in (17). Thus, (46a) and (46b) can be expressed as

$$(\mathcal{F} \mathcal{F}^H + \Psi) \Theta_S = \mathcal{F}_{\text{pres}} \quad (47a)$$

$$\Theta_Q = \mathcal{F}_{\text{past}}^H \Theta_S. \quad (47b)$$

Here, (47a) coincides with (16), and if we complex conjugate both sides of (47b) and evaluate for each matrix element  $\mathbf{Q}_n$ , we readily obtain (19). Equations (47a) and (47b) are the design equations for the MIMO DFE.

#### ACKNOWLEDGMENT

The authors would like to thank Dr. S. Andersson, Dr. U. Forssén, Mr. H. Damm, and Dr. A. Kangas at Ericsson Radio Systems AB for the opportunity to evaluate the algorithms on experimental data.

#### REFERENCES

- [1] B. D. Van Veen and K. M. Buckley, "Beamforming: A versatile approach to spatial filtering," *IEEE ASSP Mag.*, vol. 5, pp. 4–24, Apr. 1988.
- [2] M. V. Clark, L. J. Greenstein, W. K. Kennedy, and M. Shafiq, "Optimum linear diversity receivers for mobile communications," *IEEE Trans. Veh. Technol.*, vol. 43, pp. 47–56, Feb. 1994.
- [3] P. Mosen, "MMSE equalization of interference on fading diversity channels," *IEEE Trans. Commun.*, vol. COM-32, pp. 5–12, Jan. 1984.

- [4] P. Balaban and J. Salz, "Optimum diversity combining and equalization in digital data transmission with applications to cellular mobile radio—Part I: Theoretical considerations," *IEEE Trans. Commun.*, vol. 40, pp. 885–894, May 1992.
- [5] N. K. Lo, D. D. Falconer, and A. U. H. Sheikh, "Adaptive equalization for a multipath fading environment with interference and noise," in *Proc. IEEE Vehicular Technology Conf.*, Stockholm, Sweden, June 1994, vol. 1, pp. 252–256.
- [6] G. E. Bottomley and K. Jamal, "Adaptive arrays and MLSE equalization," in *Proc. 45th IEEE Vehicular Technology Conf.*, Chicago, IL, July 1995, vol. 1, pp. 50–54.
- [7] J. Winters, "On the capacity of radio communication systems with diversity in a Rayleigh fading environment," *IEEE J. Select. Areas Commun.*, vol. SAC-5, pp. 871–878, June 1987.
- [8] ———, "Optimum combining for indoor radio systems with multiple users," *IEEE Trans. Commun.*, vol. COM-35, pp. 1222–1230, Nov. 1987.
- [9] J. Salz and J. Winters, "Effect of fading correlation on adaptive arrays in digital wireless communication," in *Proc. IEEE Vehicular Technology Conf.*, St. Louis, MO, May 1993, pp. 1768–1774.
- [10] S. Verdú, "Minimum probability of error for asynchronous gaussian multiple access channels," *IEEE Trans. Inform. Theory*, vol. IT-32, pp. 85–96, Jan. 1986.
- [11] R. Lupas and S. Verdú, "Near-far resistance of multi-user detectors in asynchronous channels," *IEEE Trans. Commun.*, vol. 38, pp. 496–508, Apr. 1990.
- [12] M. K. Varanasi and B. Aazhang, "Multistage detection in asynchronous code-division multiple-access communications," *IEEE Trans. Commun.*, vol. 38, pp. 509–519, Apr. 1990.
- [13] Z. Xie, R. T. Short, and C. K. Rushforth, "A family of suboptimum detectors for coherent multiuser communications," *IEEE J. Select. Areas Commun.*, vol. 8, pp. 683–690, May 1990.
- [14] A. Duel-Hallen, "A family of multiuser decision-feedback detectors for asynchronous code-division multiple access channels," *IEEE Trans. Commun.*, vol. 43, pp. 421–434, Feb./Mar./Apr. 1995.
- [15] C. Tidestav, A. Ahlén, and M. Sternad, "Narrowband and broadband multiuser detection using a multivariable DFE," in *Proc. IEEE Int. Symp. Personal, Indoor, and Mobile Radio Communications*, Toronto, Canada, Sept. 1995, vol. 2, pp. 732–736.
- [16] C. Tidestav, "Optimum diversity combining in multi-user digital mobile telephone systems," M.S. thesis, UPTec 93094 E, Uppsala Univ., Uppsala, Sweden, Dec. 1993.
- [17] P. A. Voois and J. M. Cioffi, "Multichannel signal processing for multiple-head digital magnetic recording," *IEEE Trans. Magn.*, vol. 30, pp. 5100–5114, Nov. 1994.
- [18] A. Duel-Hallen, "Equalizers for multiple input/multiple output channels and PAM systems with cyclostationary input sequences," *IEEE J. Select. Areas Commun.*, vol. 10, pp. 630–639, Apr. 1992.
- [19] J. Karlsson, *Adaptive Antennas in GSM Systems with Non-Synchronized Base Stations*, Licentiate thesis, Royal Inst. of Technol., Stockholm, Sweden, Mar. 1998.
- [20] M. Kristensson, B. Ottersten, and D. Slock, "Blind subspace identification of a BPSK communication channel," in *Proc. 30th Asilomar Conf. Signals, Systems, and Computers*, Nov. 1996.
- [21] C. Tidestav, M. Sternad, and A. Ahlén, "Reuse within a cell—Multiuser detection or interference rejection?" Signals and Systems, Uppsala Univ., Uppsala, Sweden, Tech. Rep., May 1998.
- [22] V. Kučera, *Analysis and Design of Discrete Linear Control Systems*, Englewood Cliffs, NJ: Prentice-Hall, 1991.
- [23] J. G. Proakis, *Digital Communications*, 2nd ed. New York: McGraw-Hill, 1989.
- [24] P. Monsen, "Feedback equalization for fading dispersive channels," *IEEE Trans. Inform. Theory*, vol. IT-17, pp. 56–64, Jan. 1971.
- [25] S. Verdú, "Optimum multiuser asymptotic efficiency," *IEEE Trans. Commun.*, vol. COM-34, pp. 890–897, Sept. 1986.
- [26] C. Tidestav and E. Lindskog, "Bootstrap equalization," in *Proc. IEEE Int. Conf. Universal Personal Communications*, Florence, Italy, Oct. 1998, pp. 1221–1225.
- [27] D. Asztély, "On antenna arrays in mobile communication systems, fast fading and GSM base station receiver algorithms," M.S. thesis, Royal Inst. of Technol., Stockholm, Sweden, Feb. 1995.
- [28] T. Fulghum, K. Molnar, and A. Duel-Hallen, "The Jakes fading model incorporating angular spread," in *Proc. CISS*, Baltimore, MD, Mar. 1997.
- [29] S. Andersson, U. Forsén, J. Karlsson, T. Witzschel, P. Fischer, and A. Krug, "Ericsson/Mannesmann GSM field-trials with adaptive antennas," in *Proc. IEEE Vehicular Technology Conf.*, Phoenix, AZ, May 1997, vol. 3, pp. 1587–1591.
- [30] K. Giridhar, J. J. Shynk, A. Mathur, S. Chari, and R. P. Gooch, "Nonlinear techniques for the joint estimation of co-channel signals," *IEEE Trans. Commun.*, vol. 45, pp. 473–484, Apr. 1997.
- [31] J.-T. Chen, J.-W. Liang, H.-S. Tsai, and Y.-K. Chen, "Low-complexity joint MLSE receiver in the presence of CCI," *IEEE Commun. Lett.*, vol. 2, pp. 125–127, May 1998.



**Claes Tidestav** (S'95) was born in Enköping, Sweden, on June 4, 1969. He received the M.S. degree in engineering physics from Uppsala University, Uppsala, Sweden, in January 1994. He is currently working toward the Ph.D. degree at the Signals and Systems Group, Uppsala University.

His main research interests include multiuser detection and interference rejection for narrow-band and broadband systems and parameters estimation in cellular systems.



**Mikael Sternad** (S'83–M'86–SM'90) received the M.S. degree in engineering physics in 1981, and the Ph.D. in automatic control in 1987, both from the Institute of Technology at Uppsala University, Uppsala, Sweden.

From 1981 to 1986, he was a Teaching Assistant with the Systems and Control Group, Uppsala University. In 1987, he became an Assistant Professor, and currently, he is an Associate Professor at Uppsala University. His main research interest is signal processing applied to mobile radio communication problems.



**Anders Ahlén** (S'80–M'84–SM'90) was born in Kalmar, Sweden. He received the Ph.D. degree in automatic control in 1986 from Uppsala University, Uppsala, Sweden.

From 1984 to 1989, he was with the Systems and Control Group at Uppsala University. From 1984 to 1989, he was an Assistant Professor, and from 1989 to 1992, an Associate Professor. During 1991, he was a Visiting Research Fellow at the Department of Electrical and Computer Engineering, The University of Newcastle, Australia. In 1992, he was appointed Associate Professor in Signal Processing at Uppsala University. Since 1996, he holds the chair in Signal Processing at Uppsala University, and is also the head of the Signals and Systems Group at the same university. His research interests, which include signal processing, communications, and control, are currently focused on signal processing for wireless communications.

Prof. Ahlén is the Editor of Demodulation and Equalization for the IEEE TRANSACTIONS ON COMMUNICATIONS.